

# Coherent Population Trapping with Losses on the Sodium $D_1$ Line Hanle Effect

F. Renzoni, W. Maichen, L. Windholz and E. Arimondo <sup>(1)</sup>

*Institut für Experimentalphysik, Technische Universität Graz, A-8010 Graz, Austria*

<sup>(1)</sup> *Unità Istituto Nazionale di Fisica della Materia, Dipartimento di Fisica dell'Università,*

*I-56126 Pisa, Italia*

(March 23, 2019)

## Abstract

We consider the coherent population trapping phenomenon in a thermal sodium atomic beam. We compare the different coherent population trapping schemes that can be established on the  $D_1$  line using the Zeeman sublevels of a given ground hyperfine state. The coherent population trapping preparation is examined by means of a Hanle effect configuration. The efficiency of the coherent population trapping phenomenon has been examined in presence of optical pumping into hyperfine levels external to those of the excited transition. We show that both the contrast and the width of the coherent population trapping resonance strongly decrease when the optical pumping rate is increased. In the experiment, the loss rate due to optical pumping has been controlled by means of a laser repump of variable intensity.

PACS: 32.80.-t, 32.80.Pj, 34.50.Rk

## I. INTRODUCTION

Recently the Coherent Population Trapping (CPT) phenomenon has received a large interest, also in connection with its applications, for example the laser cooling below the recoil limit or lasing without inversion (see [1] for a review). At the beginning CPT theoretical studies were restricted to the three-level  $\Lambda$ -system [2,3], but recently they have been extended to different atom-light interaction schemes [4,5]. Despite the large amount of data available on the CPT phenomenon exploited in several atom-light interaction schemes, the features related to different level schemes and established on a given atomic species, have never been directly compared. On the other hand, the increasing interest for CPT applications requires realistic calculations taking in account processes as the loss towards the external states, the Doppler broadening of the absorbing transition, the collisions, all of them present in the experiment and determining the strength of the CPT resonance.

The main goal of the present investigation is to study the dependence of the CPT phenomenon on the atom-laser interaction parameters. In this paper we focus our attention on the level schemes that can be established on the sodium  $D_1$  line using as ground states the Zeeman sublevels of the same hyperfine component. We investigate theoretically and experimentally the CPT features associated to the different hyperfine optical transitions. As shown in Fig. 1, the hyperfine transitions composing the  $D_1$  line are:  $F_g = 1 \rightarrow F_e = 1$ ,  $F_g = 2 \rightarrow F_e = 1$ ,  $F_g = 2 \rightarrow F_e = 2$  and  $F_g = 1 \rightarrow F_e = 2$ . Within all those optical transitions, only a limited number of Zeeman sublevels contribute to the preparation of the CPT coherent superposition of states, and precisely those connected by heavy lines in Fig. 1. For instance the  $F_g = 1 \rightarrow F_e = 1$  transition contains a  $\Lambda$  system that excited by  $\sigma^+$ ,  $\sigma^-$  light produces the coherent superposition of ground states not interacting with the laser radiation. The  $F_g = 2 \rightarrow F_e = 2$  transition contains a M system that again excited by  $\sigma^+$ ,  $\sigma^-$  light produces a coherent superposition of three ground states not interacting with the laser radiation. For the transition  $F_g = 2 \rightarrow F_e = 1$  both the coherent dark superpositions listed above for the  $F_g = 1 \rightarrow F_e = 1$  and  $F_g = 2 \rightarrow F_e = 2$  transitions are present. Finally

the transition  $F_g = 1 \rightarrow F_e = 2$  is not relevant for CPT in the  $\sigma^+, \sigma^-$  light configuration, because it does not contain a coherent superposition noncoupled to the laser field.

The experiment is based on the laser excitation of a sodium atomic beam. To produce CPT in the sodium atoms and to investigate its production we have used a Hanle effect configuration. The sodium atoms are excited by monochromatic linearly polarised laser light resonant with an hyperfine optical transition; the degeneracy of the ground state Zeeman sublevels is removed by the introduction of an external magnetic field parallel to the laser propagation direction. For zero magnetic field the atomic system is optically pumped into a coherent superposition of ground states non interacting with the laser field, i.e., the dark or noncoupled state. For a fixed laser frequency, scanning the external magnetic field around the zero value, the atomic fluorescence emitted at right angles with respect to the directions of the laser field propagation and of the magnetic field exhibits a minimum at zero magnetic field with a lineshape dip typical of the Hanle/CPT phenomenon.

We have measured the contrast and the linewidth of the resonance in the Hanle/CPT lineshape versus the intensity of applied laser field. These measurements are compared to analytical and numerical analyses. For a closed optical transition the CPT process is quite straightforwardly understood and described in the frame of the optical Bloch equations. With an atomic sample in an initial uniform Zeeman distribution, the atomic preparation into the coherent superposition increases with a time constant determined by the optical pumping rate into the noncoupled state. For an open optical transition, i.e., in the presence of atomic levels external to the hyperfine transition resonant with the laser light, the atomic preparation into the coherent superposition is modified by the optical pumping into those levels. The atomic time evolution is governed by the competition between optical pumping into the noncoupled state and the optical pumping into the external hyperfine states.

We have investigated, both theoretically and experimentally, how the contrast and linewidth features of the CPT resonance depend on the optical pumping rate towards the external levels. In effect for the different hyperfine optical transitions of the sodium  $D_1$  line, owing to their different optical pumping rates, the CPT resonances have different linewidths

and contrasts. The optical pumping rate into external levels may be compensated by the application of a repumping laser of variable intensity. Thus we have studied the CPT features of a given scheme of hyperfine levels as a function of the external optical pumping loss rate by applying a repumping laser of variable intensity. Some of our results, as the narrow linewidth realized on open transitions, can be applied to the magnetometry based on coherent population trapping recently introduced by Wynands *et al* [6].

Our investigation should be compared to previous CPT studies. The more recent and detailed investigation of the CPT resonance has been performed by Ling *et al* [7]. Previous accurate studies of the Hanle effect in the ground state [8–12] have examined the lineshape dependence on the laser intensity. However none of those studies analysed the role of the different hyperfine transitions as presented here. Ling *et al* [7] have examined the role of the Doppler broadening on CPT. Their results show that in our experiment the Doppler broadening associated to the residual divergence of the sodium atomic beam has a negligible influence on the measured contrast and linewidth. Thus we have not included the Doppler broadening in our analysis. In the comparison between our data and the theoretical analysis we have discovered that our measured contrast could not reach the theoretical value because the magnetic field compensation was not accurate as required. On the contrary in the experiment by Picqué [12] the very good magnetic field compensation allowed the author to reach the contrast predicted by the theory. Thus we have used the data of ref. [12] for completing the comparison with our theoretical analysis.

In the present work Section II contains a theoretical analysis of the CPT process based on the analytical and numerical solution of the optical Bloch equations. Section III describes the experimental setup and the experimental results. Section IV contains the comparison between the theoretical analysis and the experimental results. In Section V conclusions are presented.

## II. OPTICAL BLOCH EQUATION

We consider a sodium atom interacting with a linearly polarized monochromatic laser light resonant with one of the hyperfine transition of the  $D_1$  line and propagating in the direction  $Oz$

$$\vec{E}(z, t) = \frac{\mathcal{E}}{2} \vec{\epsilon}_x e^{i(kz - \omega t)} + c.c. = \frac{\sqrt{2}\mathcal{E}}{4} (\vec{\epsilon}_{\sigma^+} + \vec{\epsilon}_{\sigma^-}) e^{i(kz - \omega t)} + c.c. \quad (1)$$

with  $\vec{\epsilon}_i$  the unit vector of the  $i$  polarization. We indicate by  $F_g \rightarrow F_e$  the transition pumped by the laser,  $F_g$  and  $F_e$  being the quantum numbers of the total angular momentum of the hyperfine levels of the  $^2S_{1/2}$  and  $^2P_{1/2}$  levels, respectively. The quantum number of the total angular momentum of the other hyperfine level of the  $^2S_{1/2}$  level will be denoted by  $F_{g'}$ . A magnetic field  $B$  is applied in the direction  $Oz$ .

For the  $z$ -axis as quantization axis, the optical Bloch equations (OBE) for the system  $F_g \rightarrow F_e$  under examination have the following form ( $|e_j\rangle = |JIF_e j\rangle$ ,  $|g_j\rangle = |JIF_g j\rangle$ ):

$$\dot{\rho}_{e_i e_j} = -[i\omega_{e_i e_j} + \Gamma_{F_e \rightarrow F_g} (1 + \alpha_{F_e \rightarrow F_g; F_{g'}})] \rho_{e_i e_j} + \frac{i}{\hbar} \sum_{g_k} (\rho_{e_i g_k} V_{g_k e_j} - V_{e_i g_k} \rho_{g_k e_j}) \quad (2a)$$

$$\dot{\rho}_{e_i g_j} = - \left[ i\omega_{e_i g_j} + \frac{\Gamma_{F_e \rightarrow F_g} (1 + \alpha_{F_e \rightarrow F_g; F_{g'}})}{2} \right] \rho_{e_i g_j} + \frac{i}{\hbar} \left( \sum_{e_k} \rho_{e_i e_k} V_{e_k g_j} - \sum_{g_k} V_{e_i g_k} \rho_{g_k g_j} \right) \quad (2b)$$

$$\dot{\rho}_{g_i g_j} = -i\omega_{g_i g_j} \rho_{g_i g_j} + \frac{i}{\hbar} \sum_{e_k} (\rho_{g_i e_k} V_{e_k g_j} - V_{g_i e_k} \rho_{e_k g_j}) + \left( \frac{d}{dt} \rho_{g_i g_j} \right)_{SE} \quad (2c)$$

The quantities  $\omega_{\alpha_i, \beta_j}$ , with  $\alpha, \beta = (e, g)$ , represent the frequency separation between the levels  $\alpha_i$  and  $\beta_j$ , including the Zeeman splittings of the ground and excited levels due to the applied magnetic field  $B$

$$\omega_{\alpha_i, \beta_j} = \frac{E_{\alpha_i} - E_{\beta_j}}{\hbar}. \quad (3)$$

$\Gamma$  is the total spontaneous emission rate for any excited level,  $\Gamma_{F_e \rightarrow F_g}$  denotes the spontaneous decay rate on the  $F_e \rightarrow F_g$  transition and  $\alpha_{F_e \rightarrow F_g; F_{g'}}$  the ratio between the spontaneous decays on the  $F_e \rightarrow F_{g'}$  and  $F_e \rightarrow F_g$  transitions. This ratio is given by [13]

$$\alpha_{F_e \rightarrow F_g; F_{g'}} = \frac{\Gamma_{F_e \rightarrow F_{g'}}}{\Gamma_{F_e \rightarrow F_g}} = \frac{2F_{g'} + 1}{2F_g + 1} \frac{\begin{Bmatrix} \frac{1}{2} & F_{g'} & \frac{3}{2} \\ F_e & \frac{1}{2} & 1 \end{Bmatrix}^2}{\begin{Bmatrix} \frac{1}{2} & F_g & \frac{3}{2} \\ F_e & \frac{1}{2} & 1 \end{Bmatrix}^2}. \quad (4)$$

The term  $\alpha_{F_e \rightarrow F_g; F_{g'}}$  describes the loss due to spontaneous decay to the ground level  $F_{g'}$  external to the transition pumped by the laser. Note that the term  $\Gamma_{F_e \rightarrow F_g}(1 + \alpha_{F_e \rightarrow F_g; F_{g'}})$  in Eqs. (2) is equal to  $\Gamma$  so that the description through  $\alpha$  evidences the role of the spontaneous decay towards external levels. For the hyperfine components of the  $D_1$  transition the values of  $\alpha$  are

$$\alpha_{F_e=1 \rightarrow F_g=1; F_{g'}=2} = 5 \quad (5a)$$

$$\alpha_{F_g=2 \rightarrow F_e=2; F_{g'}=1} = 1 \quad (5b)$$

$$\alpha_{F_g=2 \rightarrow F_e=1; F_{g'}=1} = \frac{1}{5}. \quad (5c)$$

In the dipole approximation the atom laser interaction has matrix elements

$$V_{e_i, g_j} = -\frac{\langle e_i | \vec{d} \cdot \vec{\epsilon}_x | g_j \rangle}{2} \mathcal{E}. \quad (6)$$

The spontaneous emission repopulation terms are [14,15]

$$\left( \frac{d}{dt} \rho_{g_k g_{k'}} \right)_{SE} = (2F_e + 1) \Gamma_{F_e \rightarrow F_g} \sum_{(q, q' = -F_e, +F_e), (p = -1, 1)} (-1)^{p-k-q'} \begin{pmatrix} F_g & 1 & F_e \\ -k & p & q \end{pmatrix} \rho_{e_q e_{q'}} \begin{pmatrix} F_e & 1 & F_g \\ -q' & -p & k' \end{pmatrix} \quad (7)$$

In order to examine the influence of the external levels on the Hanle/CPT resonance around zero magnetic field, we have solved numerically the time-dependent OBE with the initial condition  $\rho_{g_i, g_j}(t=0) = \frac{1}{8} \delta_{ij}$ ,  $\rho_{g_i, e_j}(t=0) = \rho_{e_i, e_j}(t=0) = 0$ . We have calculated the time-dependent fluorescence intensity emitted from the atomic system

$$I(B, t) = \Gamma \sum_{m_F = -F_e, F_e} \rho_{ee} \quad (8)$$

In our experiment on an atomic beam, we detect a signal proportional to the integrated fluorescence intensity emitted by an atom interacting with the laser light during a time  $t_f$

$$I_{\text{int}}(B) = \int_0^{t_f} I(B, t) \quad (9)$$

In the case of a closed atomic system, if the time-integrated detected signal corresponds to a long interaction times  $t_f$ , the transient initial regime produces a negligible contribution to the overall intensity. The contrast, between the maximum and the minimum of the emitted fluorescence intensity, defined as in ref. [1,16], approaches hundred percent when all the atoms are pumped into the noncoupled state. In the case of an open system the excited state occupation at the steady state is equal to zero: all population is lost because of the presence of the external state. In this case the transient regime produces the most important contribution to the integrated emitted intensity, which exhibits a Hanle/CPT resonance with contrast strongly depending on the atomic transition. Fig. 2 shows results for  $I$  versus  $B$  at different interaction times and  $I_{\text{int}}$  versus  $B$  at  $t_f = 45/\Gamma_{F_e=1 \rightarrow F_g=1}$  for the  $F_g = 1 \rightarrow F_e = 1$  hyperfine transition of the D<sub>1</sub> line, at different values of  $\alpha_{F_e \rightarrow F_g; F_g'}$ . The case  $\alpha = 0$  of (a) and (b) corresponds to an ideal close transition, the case  $\alpha_{F_e=1 \rightarrow F_g=1; F_g'=2} = 5$  of (c) and (d) corresponds to the real  $F_g = 1 \rightarrow F_e = 1$  transition of the D<sub>1</sub> line. In (a) and (b) for the case of a closed atomic system, where  $\alpha_{F_e \rightarrow F_g; F_g'} = 0$ , the time-dependent fluorescence intensity exhibits a sharp and well pronounced Hanle/CPT resonance around zero magnetic field. The contrast of  $I_{\text{int}}$  increases with the interaction time and results around 100 % at larger interaction times. In (c) and (d) a large loss towards external states produces a reduced intensity  $I$ , and a smaller contrast in the integrated intensity  $I_{\text{int}}$ . The limiting value for the contrast observed on  $I$  is 100 percent independently of the loss rate and is reached at interaction times shorter than in the case of a closed system, because only those atoms already in the noncoupled state contribute to the contrast, the remaining ones been pumped into the external states. The integrated fluorescence  $I_{\text{int}}$  is obtained summing up the contributions at different times, and those at earlier times have a larger weight on the sum. Also for an open system the contrast increases with the interaction time, reaching a value smaller than 100 % at larger interaction times.

Fig. 3 shows the results for the integrated fluorescence intensity  $I_{\text{int}}$  in the case of the real open transitions of sodium, for a choice of experimental parameters corresponding to the conditions of the experimental investigation. The different contrast of the Hanle/CPT

resonance for the different hyperfine transitions is quite evident. A large contrast is obtained for the  $F_g = 2 \rightarrow F_e = 1$  transition with the smallest value of losses towards external states.

The results of Figs. 2,3 show that the loss towards the external states modifies strongly also the linewidth. In Fig. 2 the resonance linewidth for the case of  $\alpha_{F_e=1 \rightarrow F_g=1; F_g=2} = 5$  is much narrower than the linewidth for the case  $\alpha = 0$ . In Fig 3 the real hyperfine transitions are directly compared and once again open transitions with a larger loss towards external states have a more narrow resonance. The comparison between different hyperfine transitions is not straightforward because the matrix element  $V_{e,g}$  of the atom-laser interaction between excited and ground states depends on the hyperfine levels, and furthermore in the system  $F_g = 2 \rightarrow F_e = 1$  two noncoupled states are present. However the CPT analysis for a closed symmetrical  $\Lambda$  system performed in the basis of the coupled and noncoupled states is very useful for the interpretation. In that analysis [1,16], in absence of ground state relaxation, at the steady state the linewidth of the CPT resonance is determined by the loss rate  $\Gamma'$  of the coupled state, with  $\Gamma' = V_{e,g}/(\hbar^2\Gamma_{\text{exc}})$ ,  $\Gamma_{\text{exc}}$  being the excited state lifetime. In Fig. 2, the main difference between the closed, in (a) and (b), and open, in (c) and (d), systems is the excited state lifetime, with  $\Gamma_{\text{exc}} = \Gamma_{1 \rightarrow 1}$  in the first case, and  $\Gamma_{\text{exc}} = \Gamma_{1 \rightarrow 1}\alpha_{1 \rightarrow 1;2}$  in the second case. An increase in that lifetime produces a smaller  $\Gamma'$  and a more narrow CPT resonance, as observed in the figure for both  $I$  and  $I_{\text{int}}$ . It should be noted that in an open system the coupled-noncoupled approach applied to states without population because of the optical pumping towards external states is not really meaningful.

The narrow linewidths obtained in Fig. 3 have a different explanation, because for the real  $D_1$  line hyperfine transitions the excited states have the same lifetime  $\Gamma$ , whichever Zeeman/hyperfine component. The narrow resonances are obtained in the curve of  $I_{\text{int}}$  versus  $B$  and the contribution of  $I$  at different interaction times should be considered. They arise because of the simultaneous action of the pumping into the noncoupled nonabsorbing state and of the optical pumping towards external states. The optical pumping towards external states is less efficient whenever the optical pumping in the noncoupled states is more efficient: in the noncoupled state the atomic wavefunction has no contribution of



excited state, whence the atom does not decay towards the external states. Thus the narrow CPT resonance, being produced by the contribution of only those atoms remaining in the noncoupled state and nondecaying towards the external states, is a consequence of an atomic selection.

### III. EXPERIMENTAL SET-UP

The experimental setup is shown in Fig. 4. We used a single mode CW dye laser; the light polarization was linear and the propagation direction orthogonal to the thermal sodium atomic beam. An external magnetic field was applied parallel to the laser beam propagation direction. Magnetic field Helmholtz coils, applied around the atom-laser interaction region, were driven by a programmable power supply in order to produce a linear scan of the magnetic field. The earth magnetic field was compensated to better than 0.05 G by additional pairs of Helmholtz coils. By tuning the laser to different hyperfine optical transitions of the sodium D<sub>1</sub> line, we excited different atomic configurations. The laser frequency was tuned to the center of the homogeneous hyperfine absorption profile. The fluorescence signal emitted by the sodium atoms at right angles with respect to the directions of the laser field propagation and of the magnetic field was detected through a photomultiplier and recorded by means of a lock-in amplifier and a standard data acquisition system. In our experiment the interaction time was of the order of few  $\mu\text{s}$ , to be compared to the  $3P_{1/2}$  excited state lifetime of sixteen  $\text{ns}$ .

### IV. EXPERIMENTAL RESULTS AND COMPARISON WITH THEORY

Examples of the time integrated fluorescence signals recorded on the different hyperfine transitions are shown in Fig. 5. Three of the four transitions on the D<sub>1</sub> line exhibit the Hanle/CPT typical dip. The transition  $F_g = 1 \rightarrow F_e = 2$  does not exhibit any dip because there are no noncoupled states into which the atom could be pumped. The dip contrasts for the other three transitions,  $F_g = 1 \rightarrow F_e = 1$ ,  $F_g = 2 \rightarrow F_e = 1$ ,  $F_g = 2 \rightarrow F_e = 2$ , are

very different. The dip for the transition  $F_g = 2 \rightarrow F_e = 1$  is very pronounced, and the corresponding contrast is large. The contrasts of the dips associated with the transitions  $F_g = 1 \rightarrow F_e = 1$  and  $F_g = 2 \rightarrow F_e = 2$  are smaller. The observed behaviours correspond to those predicted by the analysis and shown in Fig. 2. The hyperfine transitions with a larger loss factor  $\alpha$  towards external states present a more narrow Hanle/CPT resonance. However it should be noted that different hyperfine transitions cannot be directly compared as already discussed.

The FWHM linewidth and the contrast of the Hanle/CPT resonance for the various hyperfine transitions have been studied as a function of the laser intensity. The experimental results are shown in Fig. 6 and 7a. The experimental results of Figs. 6 and 7a for the linewidth and contrast of the Hanle/CPT resonance have been compared to the theoretical numerical analysis. The theory predicts an increase of the linewidth and contrast with the applied laser intensity, as observed in the experiment. However the maximum contrast achieved in our experimental observations is lower than that predicted by the theory. For instance for the  $F_g = 2 \rightarrow F_e = 1$  hyperfine transition, the maximum theoretical contrast is sixtyseven percent, while the measured value of the maximum contrast on that transition is around fifty percent. In order to examine more carefully the comparison between theory and experiments, our theoretical analysis has been applied also to the Hanle/CPT measurements published by Picqué [12] in an experimental configuration very similar to the present one, on the  $F_g = 2 \rightarrow F_e = 1$  hyperfine transition of the sodium D<sub>1</sub> line as a function of the applied laser field intensity. The contrast of the Hanle/CPT resonances, as derived from the five curves published in [12], and the results of a theoretical analysis for the interaction times of that reference are reported in Fig. 7b. In this case the agreement between our theory and the experimental results is very good, confirming the validity of the theoretical approach. The experiment of [12] reported a compensation of the stray magnetic fields within 10 mG over the whole atom-laser interaction volume. Thus our failure to reproduce the theoretical contrast is produced by an imperfect compensation of the magnetic field in our apparatus. More precisely owing to the presence of some magnetic field gradient present

in the atom-laser interaction region, the magnetic field could not be compensated over the whole interaction region through our Helmholtz coils.

For the  $D_1$  excitation on sodium atoms none of the hyperfine optical transitions is closed. However experimentally a closed-like situation can be realized through the application of a repumping laser which compensates the losses term  $\dot{\rho}_{e_i e_i} = -\alpha_{F_e \rightarrow F_g; F_g'} \Gamma_{F_e \rightarrow F_g} \rho_{e_i e_i}$  for the population decay. We examined, for a given transition, the dependence of contrast and linewidth on the population loss rate, by applying a repumping laser to partially compensate the losses towards external states. Varying the intensity of the repumping laser it was possible to study the features of the CPT resonance as a function of the rate of population losses. Obviously the repumping transition should be chosen in order to not produce an additional noncoupled coherent superposition. In the case of the sodium  $D_1$  line the most favourable transition for this study is the  $F_g = 2 \rightarrow F_e = 2$  transition because the transition  $F_g = 1 \rightarrow F_e = 2$ , without noncoupled state, as verified by the record in Fig. 5d, can be used for repumping. The CPT results in presence of a repumping laser are reported in Fig. 8: it is clearly visible that the contrast and the width of the CPT resonance increase for increasing power of the repumping laser, i.e., for a decreasing rate of population losses. These experimental results can be compared to the theoretical ones of Fig. 2. The presence of a repumping laser, compensating for the losses towards external states, is equivalent to a longer lifetime of the excited state. Thus starting from the configuration of an open system as in Fig. 2(b) in absence of the repumping laser, its application produces an effective closed system as in Fig. 2(a). It should be noted that the repumping laser does not compensate for the decay rate of the optical coherences. However after preparation of the atoms in the noncoupled states, the optical coherences are zero and their decay is not relevant for the atomic preparation.

## V. CONCLUSIONS

The CPT phenomenon on the sodium  $D_1$  line has been investigated by means of an Hanle effect configuration comparing different level schemes ( $\Lambda$  and  $M$ ) and studying the influence of the losses towards external states. Different atom-laser interaction schemes involving as ground states the sublevels of the same hyperfine component have been considered. On the sodium  $D_1$  line the relevant transitions are  $F_g = 1 \rightarrow F_e = 1$ ,  $F_g = 2 \rightarrow F_e = 1$ ,  $F_g = 2 \rightarrow F_e = 2$ . As original contribution of the present investigation we have investigated CPT in atomic configurations not closed for spontaneous emissions decay. We have demonstrated that CPT may be realized on those open transitions with an efficiency decreasing with the amount of spontaneous emission towards external states. Because in the  $D_1$  line the different level configurations correspond to different rates of population losses, the features, i.e., width and contrast, of the Hanle/CPT resonance depend on the explored transition. A careful study of the dependence of the width and contrast of the Hanle/CPT dip on the interaction parameters has been performed. A numerical analysis of the density matrix equations confirms most experimental observations, except that the maximum contrast is lower than the expected one because of the not perfect compensation of the magnetic field in the experiment. However our numerical analysis is in agreement with the contrast measured in a previous experiment [12] where a very good magnetic field compensation was applied. The experimental data show that the contrast of the Hanle/CPT dip is less than 100 %. It depends strongly on the population loss rate and it can be controlled by means of a repumping laser that compensates the rate of population losses towards the external levels. The contrast of the Hanle/CPT resonance is only weakly affected by the small Doppler broadening associated to the atomic beam.

Note that in the regime of very large saturation, the power broadening of the spectral lines does not allow the interpretation of the experiment as a pure  $F_g \rightarrow F_e$  transition with losses on  $F_{g'}$ . Let us consider for example the case of  $F_g = 1 \rightarrow F_e = 1$  ( $\Lambda$ -scheme). At large laser saturation the absorption lines  $F_g = 1 \rightarrow F_e = 1$  and  $F_g = 1 \rightarrow F_e = 2$  are excited

simultaneously. Thus we don't have a pure  $\Lambda$ -system but a  $\Lambda + W$  system where the states are not completely dark for the laser absorption.

## VI. ACKNOWLEDGMENTS

This work has been partially supported by the Austrian Science Foundation No. S 6508.

## REFERENCES

- [1] E. Arimondo, in *Progress in Optics* ed. E. Wolf, vol. 35 (Elsevier, Amsterdam, 1996) p. 257.
- [2] E. Arimondo and G. Orriols, *Lett. Nuovo Cimento* **17**, 333 (1976).
- [3] H.R. Gray, R.W. Whitley, and C.R. Stroud Jr, *Opt. Lett.* **3**, 218 (1978).
- [4] V.S. Smirnov, A.M. Tumaikin, and V.I. Yudin, *Sov. Phys. JETP* **69**, 913 1989.
- [5] F. Papoff, F. Mauri, and E. Arimondo *J. Opt. Soc. Amer. B* **9**, 321 (1992).
- [6] R. Wynands, S. Brandt, A. Nagel and D. Meschede, Technical Digest IQEC'96 (Optical Society of America, Washington, USA, 1996) paper TuL62, and Technical Digest CLEO/Europe-EQEC'96, (Optical Society of America, Washington, USA, 1996) paper QThJ1.
- [7] H.Y. Ling, Y.-Q. Li, and M. Xiao *Phys. Rev. A* **53** 1014 (1996).
- [8] J.C. Lehmann and C. Cohen-Tannoudji, *Comptes Rend. Ac. Sci. Paris* **258**, 4463 (1964); J. Dupont-Roc, S. Haroche, and C. Cohen-Tannoudji, *Phys. Lett.* **28A**, 638 (1969); C. Cohen-Tannoudji, J. Dupont-Roc, S. Haroche, and F. Laloë, *Rev. Phys. Appl.* **5**, 95 (1970); C. Cohen-Tannoudji, in *Frontiers in Laser Spectroscopy* vol. 1 eds. R. Balian, S. Haroche and S. Liberman (North Holland, Amsterdam, 1977) p. 3.
- [9] W. Rasmussen, R. Schieder, and H. Walther, *Opt. Comm.* **12**, 315 (1974).
- [10] R. Schieder and H. Walther, *Z. Phys.* **270**, 55 (1974).
- [11] H. Brand, W. Lange, J. Luther, B. Nottbeck, and R. Schröder, *Opt. Comm.* **13**, 286 (1975).
- [12] J.L. Picqué, *J. Phys. B: At. Mol. Phys.* **11**, L59 (1978).
- [13] I.I. Sobel'man, in *Atomic Spectra and Radiative Transitions*, Vol. 1 of Springer Series

in Chemical Physics (Springer, Berlin, 1979).

[14] W. Happer, Rev. Mod. Phys. **44**, 169 (1972).

[15] A. Omont, Progr. Quant. Electr. **5**, 69 (1977).

[16] E. Arimondo, Phys. Rev. A **54**, 2216 (1996).

## FIGURES

FIG. 1. Different CPT schemes that can be established on the hyperfine components of the sodium D<sub>1</sub> line through excitation by  $\sigma_+$ ,  $\sigma_-$  laser lights.

FIG. 2. Theoretical results for the time dependent intensity  $I$  versus time  $t$  and integrated fluorescence intensity  $I_{\text{int}}$  at  $t_f = 45$  for the  $F_g = 1 \rightarrow F_e = 1$  hyperfine transition in correspondence of different values of the loss parameter  $\alpha_{F_e=1 \rightarrow F_g=1, F_g'=2}$ . In (a) and (b)  $\alpha_{F_e=1 \rightarrow F_g=1, F_g'=2} = 0$ , i.e. a hypothetical closed transition; in (c) and (d)  $\alpha_{F_e=1 \rightarrow F_g=1, F_g'=2} = 5$  as for the real hyperfine transition of the D<sub>1</sub> line. The time  $t$  and  $t_f$  are measured in units of  $1/\Gamma_{F_e=1 \rightarrow F_g=1}$ . The laser intensity is 26 mW/cm<sup>2</sup>.

FIG. 3. Theoretical results for the integrated fluorescence intensity  $I_{\text{int}}$  at  $t_f = 45/\Gamma_{F_e=1 \rightarrow F_g=1}$  for the real (open) transitions of the sodium D<sub>1</sub> line, calculated for the laser intensity of 26 mW/cm<sup>2</sup>. (a) corresponds to the transition  $F_g = 1 \rightarrow F_e = 1$ , (b) to  $F_g = 2 \rightarrow F_e = 1$ , and (c) to  $F_g = 2 \rightarrow F_e = 2$ .

FIG. 4. Experimental setup for the investigation of the Hanle/CPT resonance on a sodium atomic beam for the different hyperfine transitions on the D<sub>1</sub> line.

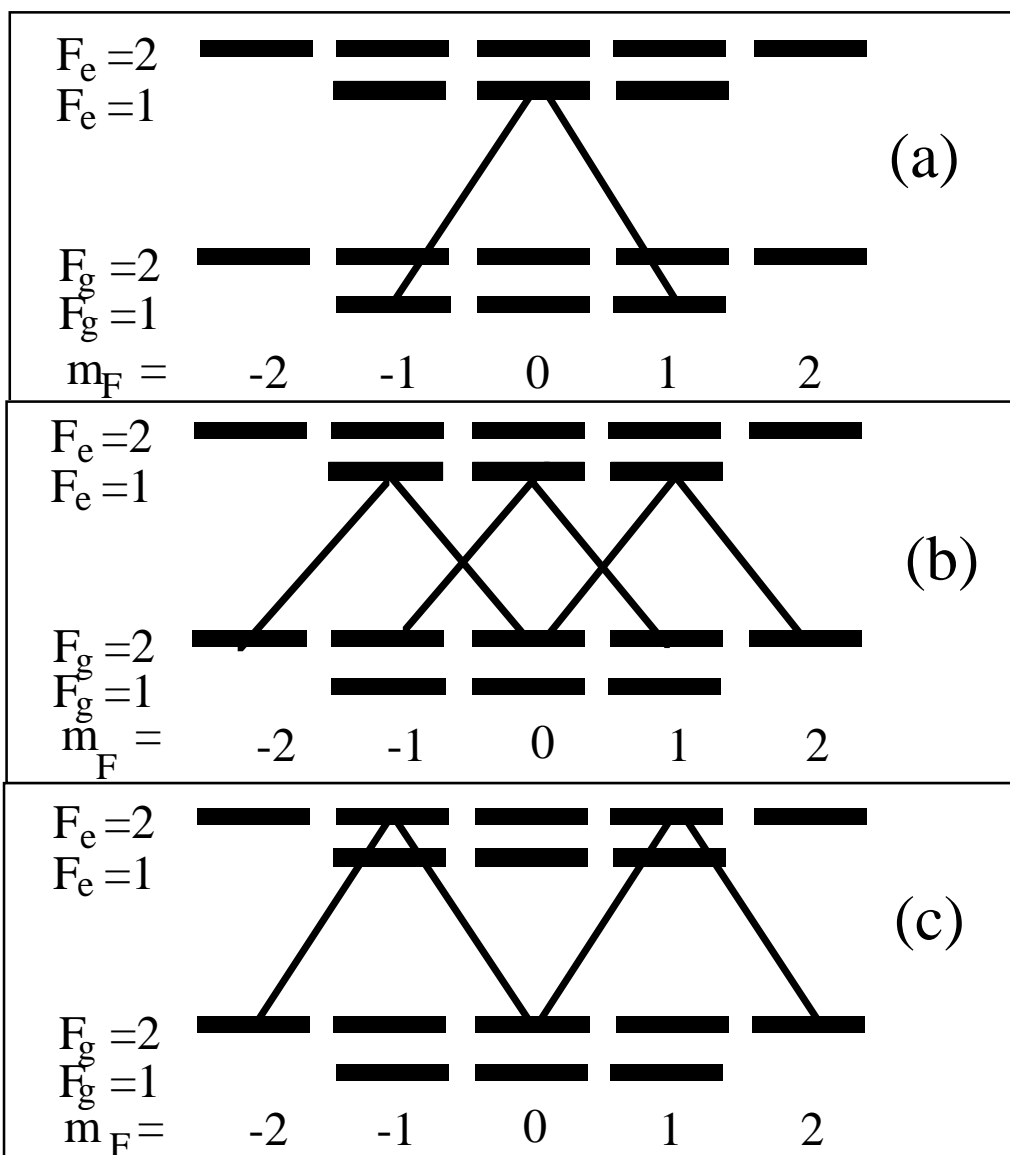
FIG. 5. Experimental results for the fluorescence intensity  $I_{\text{int}}$  as a function of the magnetic field  $B$  on the different hyperfine transitions with no repumping laser. The interaction time is  $\simeq 4.5\mu\text{s}$ . Laser intensity  $I_L = 26$  mW/cm<sup>2</sup> in all the data sets.

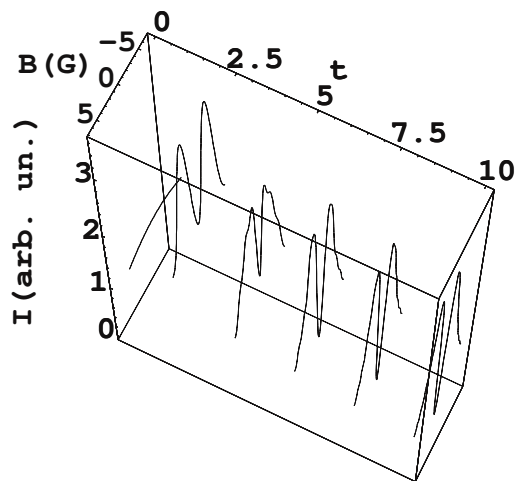
FIG. 6. Experimental results for the FWHM linewidth of the Hanle/CPT resonance for the different hyperfine transitions as a function of the laser intensity. Black triangles correspond to laser excitation on the transition  $F_g = 2 \rightarrow F_e = 2$ , while open squares to  $F_g = 1 \rightarrow F_e = 1$  and closed circles to  $F_g = 2 \rightarrow F_e = 1$ . Typical error bars are marked.



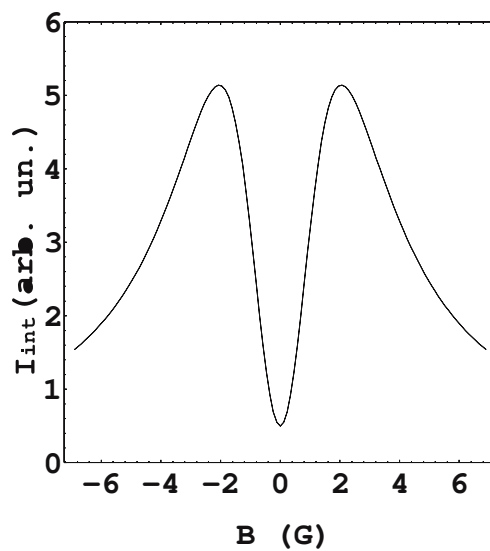
FIG. 7. In (a) experimental results for the contrast of the Hanle/CPT resonance for the different hyperfine transitions as a function of the laser intensity. Black triangles correspond to the transition  $F_g = 2 \rightarrow F_e = 2$ , open squares to  $F_g = 1 \rightarrow F_e = 1$  and closed circles to  $F_g = 2 \rightarrow F_e = 1$ . Typical error bars are marked. In (b) experimental results for the  $F_g = 2 \rightarrow F_e = 1$  transition from ref. [12] for the contrast of the Hanle/CPT resonance as a function of the laser intensity. Laser intensity derived from [12]; error bar of the contrast estimated on the figures of that reference.

FIG. 8. Experimental results for the fluorescence intensity as a function of the applied magnetic field, with one laser tuned to the transition  $F_g = 2 \rightarrow F_e = 2$  to establish the M-scheme; another laser tuned to the transition  $F_g = 1 \rightarrow F_e = 2$  to repump the atoms. The intensity of the laser used to establish the M-scheme was  $I_L = 250 \text{ mW} / \text{cm}^2$ . The intensity of the repumping laser was in (a)  $I_R = 0$ , in (b)  $I_R = 20 \text{ mW}/\text{cm}^2$ , (c)  $I_R = 200 \text{ mW}/\text{cm}^2$ .

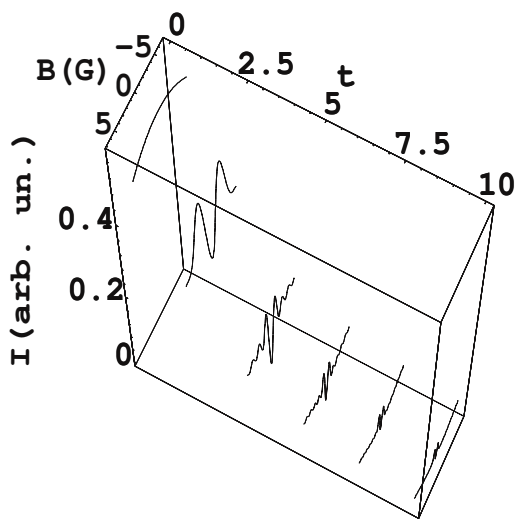




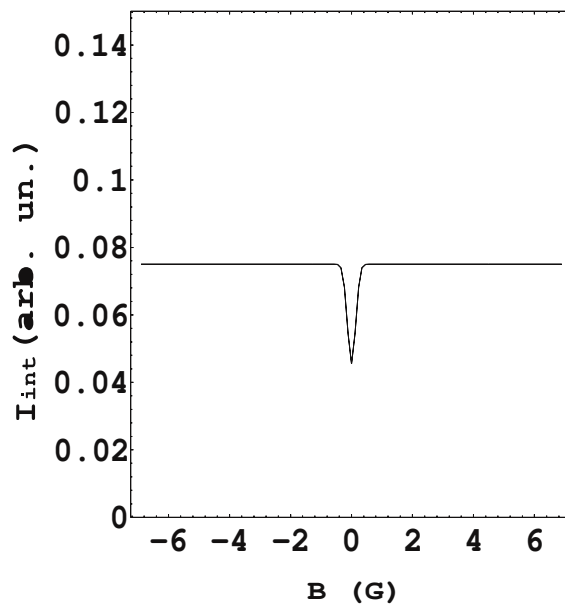
(a)



(b)

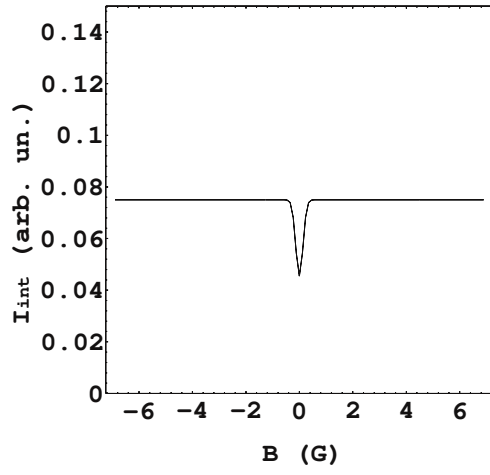


(c)

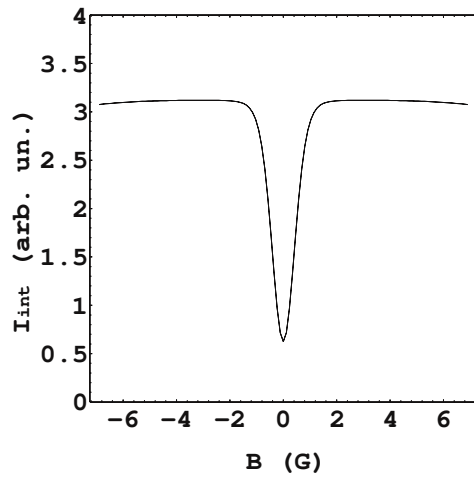


(d)

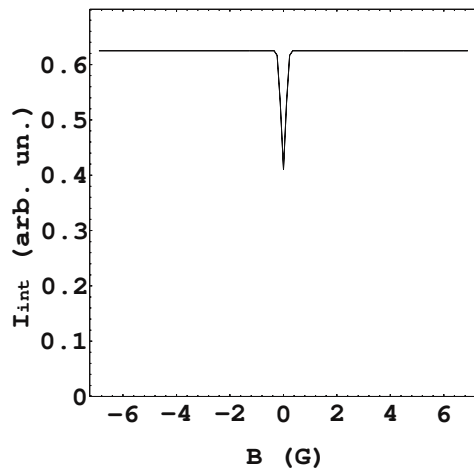
(a)

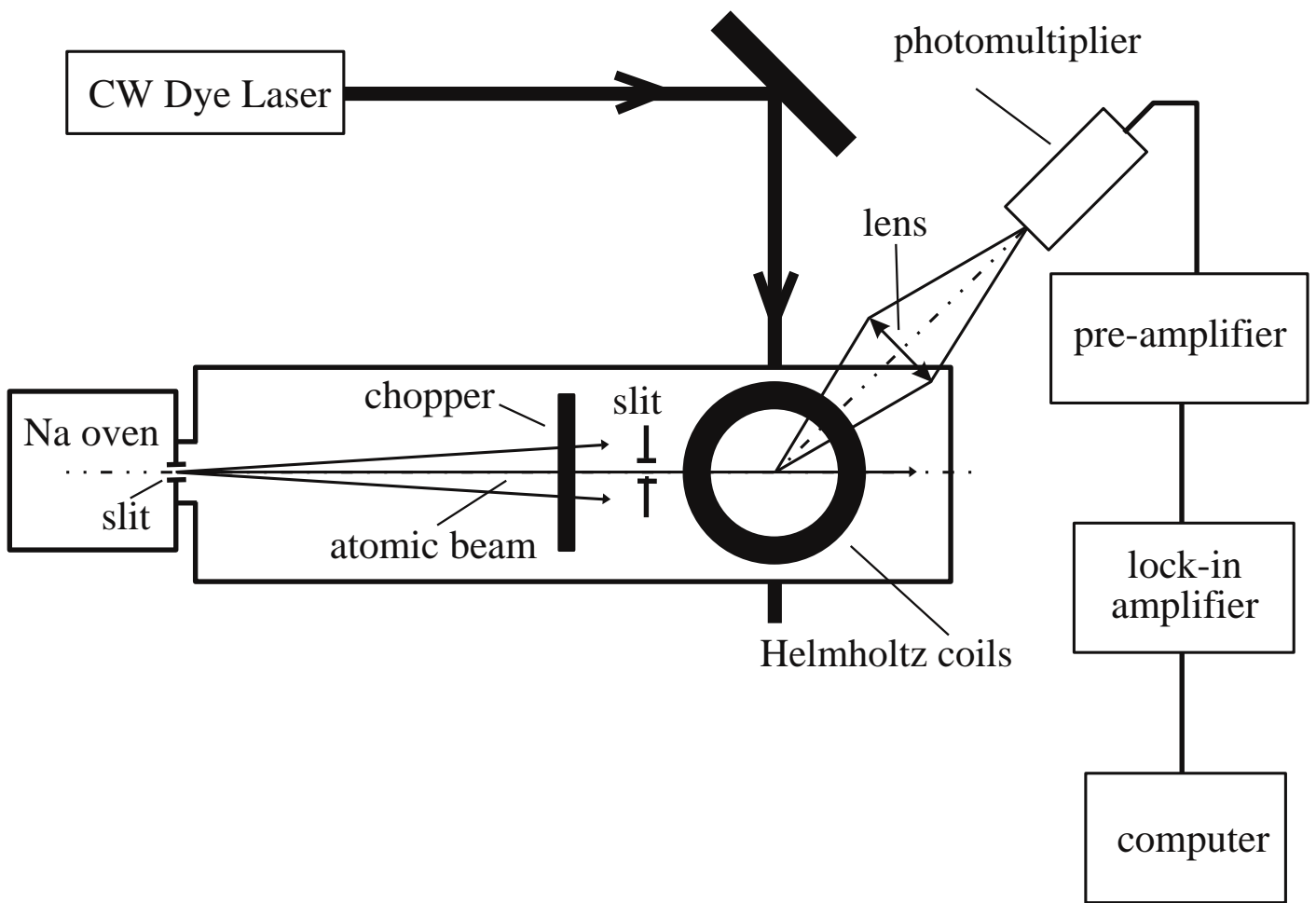


(b)

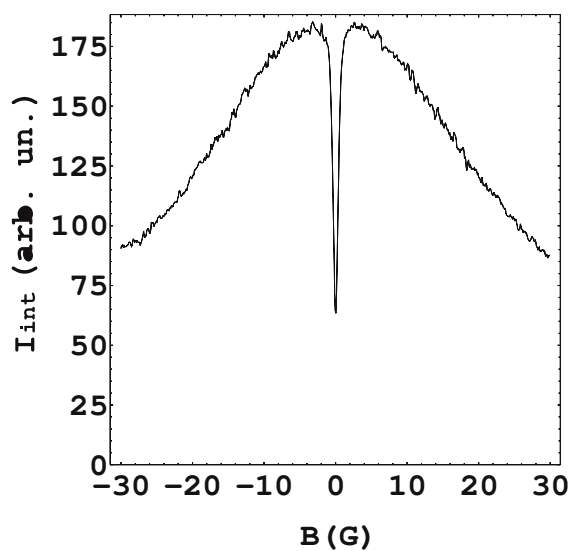


(c)

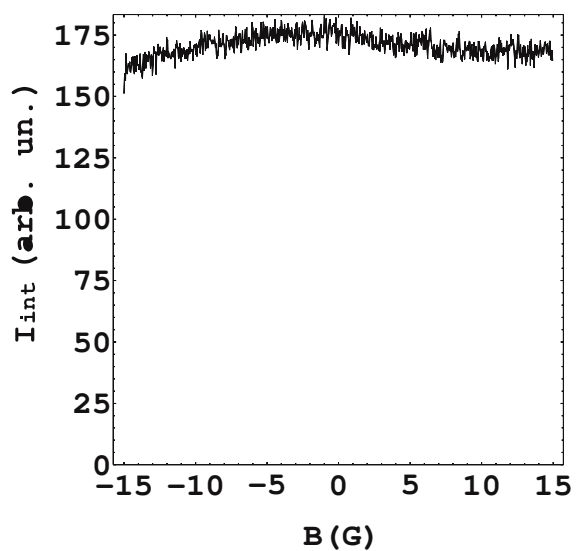




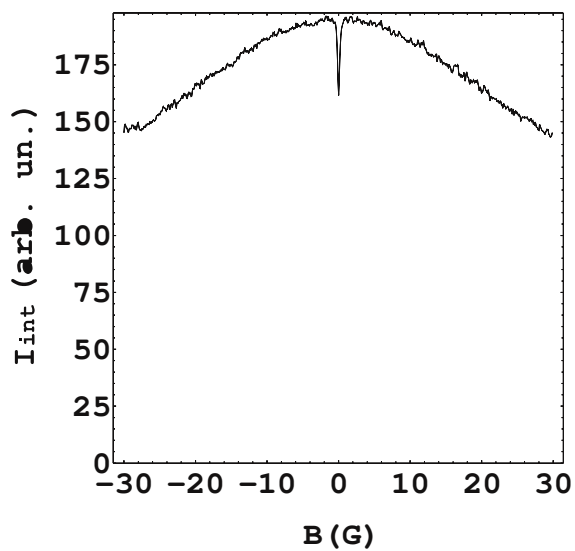
$F_g=2 \rightarrow F_e=1$



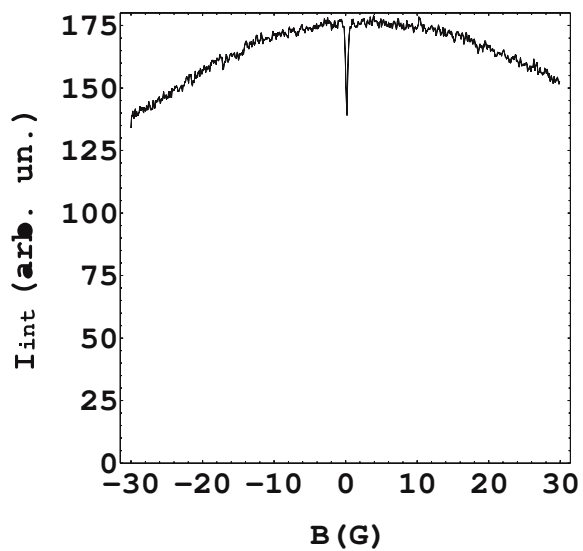
$F_g=1 \rightarrow F_e=2$

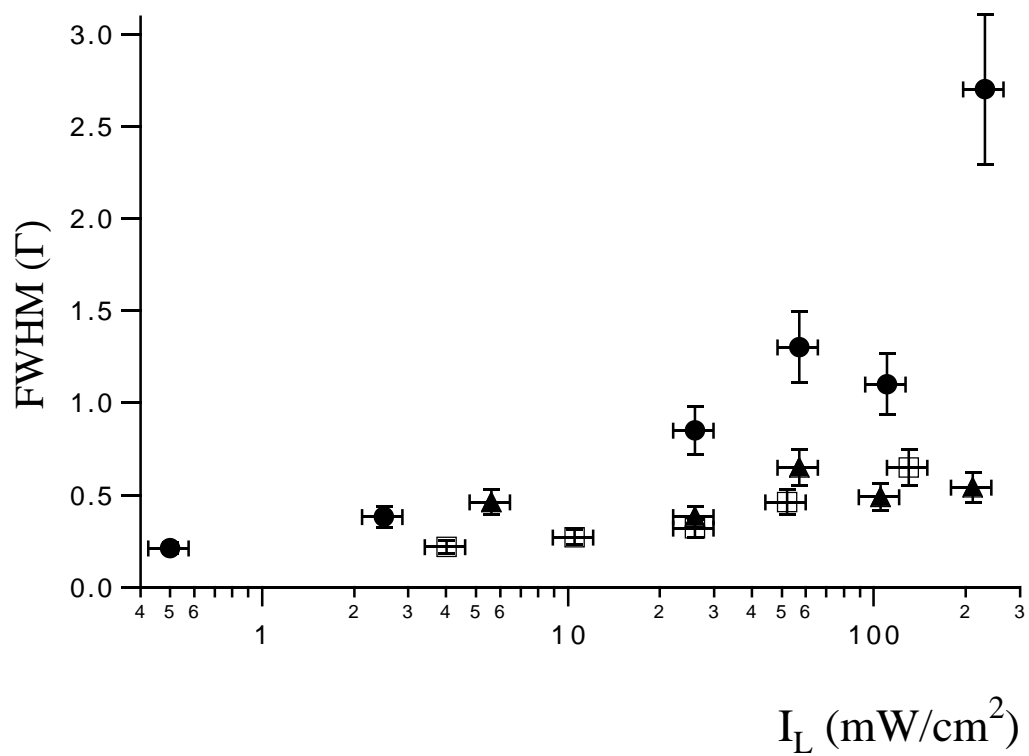


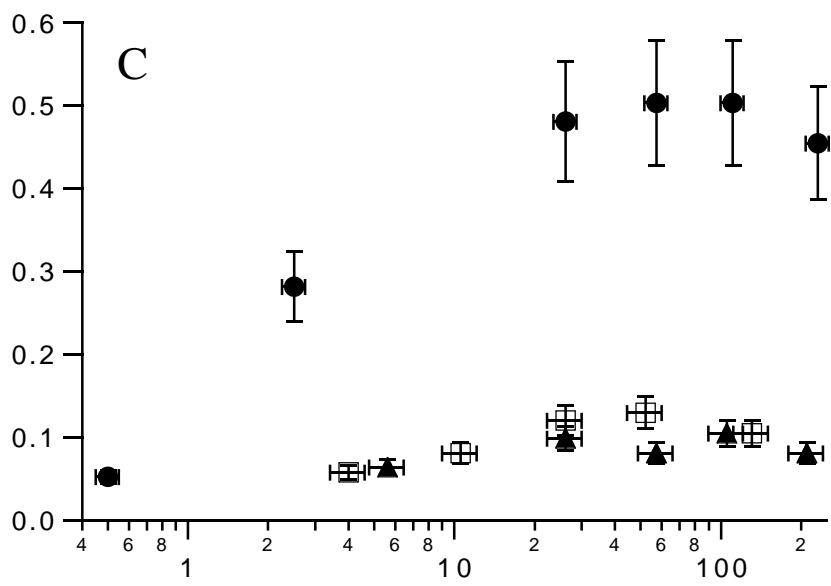
$F_g=2 \rightarrow F_e=2$



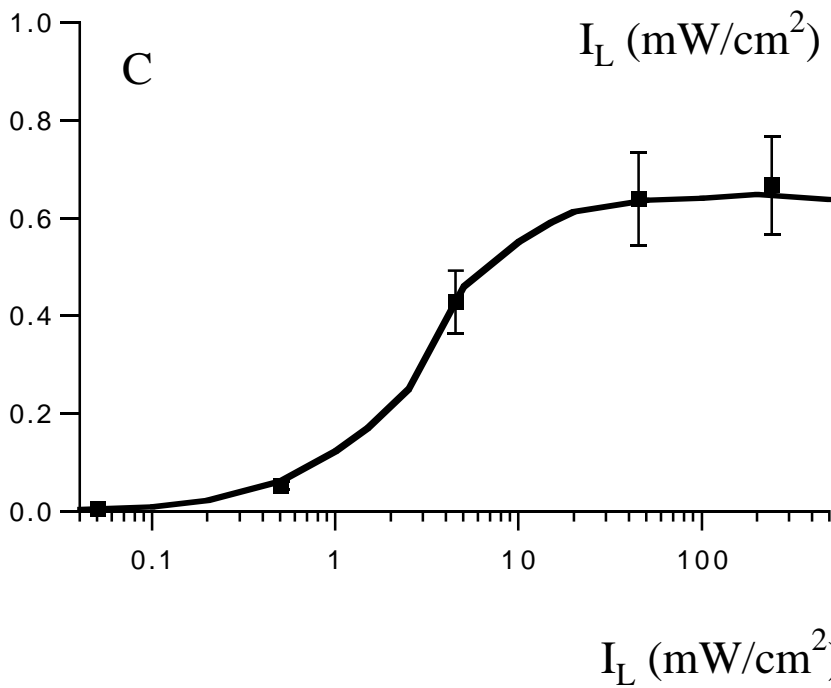
$F_g=1 \rightarrow F_e=1$







(a)



(b)



